ADVANCED FUNCTIONAL MATERIALS
www.afm-journal.de

A Photon-Fueled Gate-Like Delivery System Using i-Motif DNA Functionalized Mesoporous Silica Nanoparticles

Dinggeng He, Xiaoxiao He, Kemin Wang, Jie Cao, and Yingxiang Zhao*

A novel photon-fueled gate-like mesoporous silica nanoparticles (MSN)-based delivery system is reported. In this system, the malachite green carbinol base (MGCB) is immobilized on the nanochannel wall of MSN as a light-induced hydroxide ion emitter and i-motif DNA is grafted on the surface of MSN as a cap. Photoirradiation with 365 nm wavelength UV light makes MGCB molecules dissociate into malachite green (MG) cations and OH^- ions, which induce the i-motif DNA to unfold into the single-stranded form due to the increase of the pH in the solution. Therefore, the pores are uncapped and the entrapped guest molecules are released. After the light is turned off, the MG cations recombine with the OH^- ions and return to the MGCB forms. The pH value thus decreases and the single-stranded DNA switches back to i-motif structure to cap the pore again. Because of the photon-fueled MGCB-dependent DNA conformation changes, the i-motif DNA-gated switch can be easily operated by turning the light on or off. Importantly, the opening/closing protocol is highly reversible and a partial cargo release can be easily achieved at will. This proof-of-concept may promote the application of DNA in the controlled release and can also provide a way to design various photon-fueled controlled-release systems using a combination of some photoirradiated pH-jump systems and other kinds of pH-sensitive linkers.

1. Introduction

With the distinctive characteristics of stable mesostructure, biocompatibility, large loading capacity, and ease of surface functionalization, mesoporous silica nanoparticles (MSN) have attracted great attention in a stimuli-responsive capped/gated release mechanism.[1] To date, several stimuli-responsive strategies including photoirradiation,[2] pH,[3] temperature,[4] competitive binding,[5] enzymes,[6] and redox activation[7] have been applied as "triggers" for uncapping the pores. Most of the reported systems have been constructed by various pore-blocking caps such as nanoparticles,[8] organic molecules,[9] and supramolecular assemblies[10] and so on. Despite enormous research progress in this field, many of the existing cap systems still have presented disadvantages in terms of irreversibility, poor biocompatibility, toxicity of the capping agents, etc.

Oligonucleotide is an attractive material for the design of stimuli-responsive delivery systems owing to their conformational polymorphism, good biocompatibility and robust physicochemical nature. Many MSN-based stimuli-responsive release systems with nucleic acids as caps have been constructed. In these systems, the conformational switch of nucleic acids has been driven by a contact model triggers involving complementary DNA strands,[11] acids/bases,[12] enzymes,[13] or target molecules.[14] The contact mode shows an excellent controlled release behavior through interactions between nucleic acids and stimulators. This DNA-based model trigger requires a direct contact between delivery system and stimulus, and as a result, limits the response rate and degree of control of designed controlled release system. Moreover, it can not be applied to reactions in complex systems or customizing environments. In contrast, photoirradiation as a noninvasive trigger is more convenient and desired strategy for the regulation of DNA conformation. As references reported, there are mainly two kinds of photoregulated of DNA conformation. One kind of them is the photoregulation of modified DNA conformation by introducing the photo-sensitive group into DNA strands to serve as an artificial base pair or the photolabile protection groups to mask the Watson–Crick base pairing.[15] The other is the light-induced conformational switch of natural DNA through a photoirradiated pH-jump system.[16] In this strategy, the light-induced DNA conformational switch between close-packed quadruplex and random-coil structures is achieved by malachite green carbinol base (MGCB) as a reversible photoirradiated pH-jump system. It can undergo multiple cycling of DNA conformation by turning the UV light on and off alternately in noncontact mode. However, light-driven conformational alteration of DNA for application in the field of controlled release has not been reported.

Herein, we have sought to take advantage of this unique feature to rationally design a novel photon-fueled molecular gate-like delivery system, employing MGCB to be immobilized into

Dr. D. G. He, Prof. X. X. He, Prof. K. M. Wang, J. Cao, Y. X. Zhao
State Key Laboratory of Chemo/Biosensing and Chemometrics
Key Laboratory for Bio-Nanotechnology and Molecular Engineering of Hunan Province
College of Chemistry and Chemical Engineering
College of Biology, Hunan University
Changsha 410082, P. R. China
E-mail: kmwang@hnu. edu.cn

DOI: 10.1002/adfm.201201343

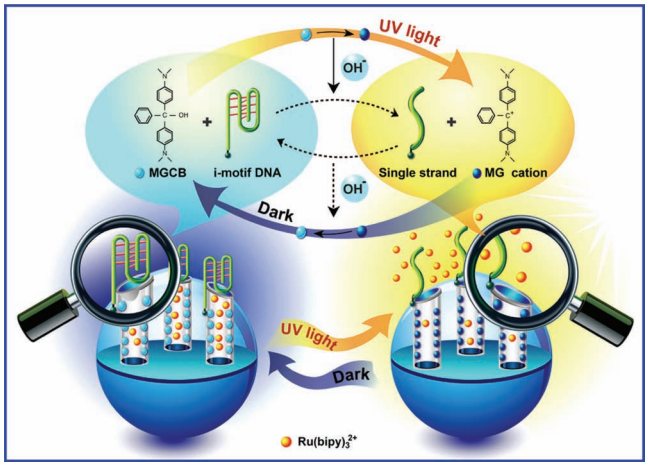

Scheme 1. Schematic representation of photon-fueled release of guest molecules from the pores of MSN capped with i-motif DNA (DNA1). The conformational switch of DNA1 was associated with the on and off phases of UV light through the translation of light-induced hydroxide-group release by MGCB.

the nanochannel walls of MSN as a light-induced hydroxide ion emitter and i-motif DNA (DNA1) to be grafted on the surface of MSN as a cap material. The obtained system is denoted as MGCB@MSN-DNA1. The primary motivation for employing DNA1 as a cap material is based on the fact that it is nontoxic, hydrophilic, and exhibits reversible response to pH (it folds into i-motif form at pH = 5.0 but rapidly unfolds into single strand at pH = 8.0).[17] The working principle of the photon-fueled controlled-release system is illustrated in **Scheme 1**. In this design, the initial solution containing MGCB@MSN-DNA1 shows a slightly acidic pH value (pH = 5.0) that facilitates the formation of i-motif structures by one or association of two or more single-stranded DNA1 to cap the pores. In the presence of 365 nm UV light, MGCB molecules immobilized into the nanochannels of MSN dissociate into malachite green (MG) cations and OH^- ions, which lead to an increase in the pH value. As a result, the i-motif quadruplex structures unfold into single-stranded forms due to deprotonation of the C:C$^+$ base pairs and the pores are uncapped, resulting in a rapid release of the entrapped cargo from the pore voids into the aqueous solution. After the light is turned off, the MG cations recombine with the OH^- ions and return to the MGCB forms to complete the cycle. Thus, the pH value decreases and the single-stranded DNA1 switches back to i-motif form again. Accordingly, the conformational alterations of DNA1 and the closed and open states of the gated system can be cycled by turning the UV light on and off alternately.

2. Results and Discussion

For the design of the stated gate-like delivery system above, we first synthesized chlorine-functionalized MSN (MSN-Cl) with a MCM–41–type mesoporous structure. The obtained particles were characterized by transmission electron microscopy (TEM), powder X-ray diffraction (XRD), and N_2 adsorption–desorption

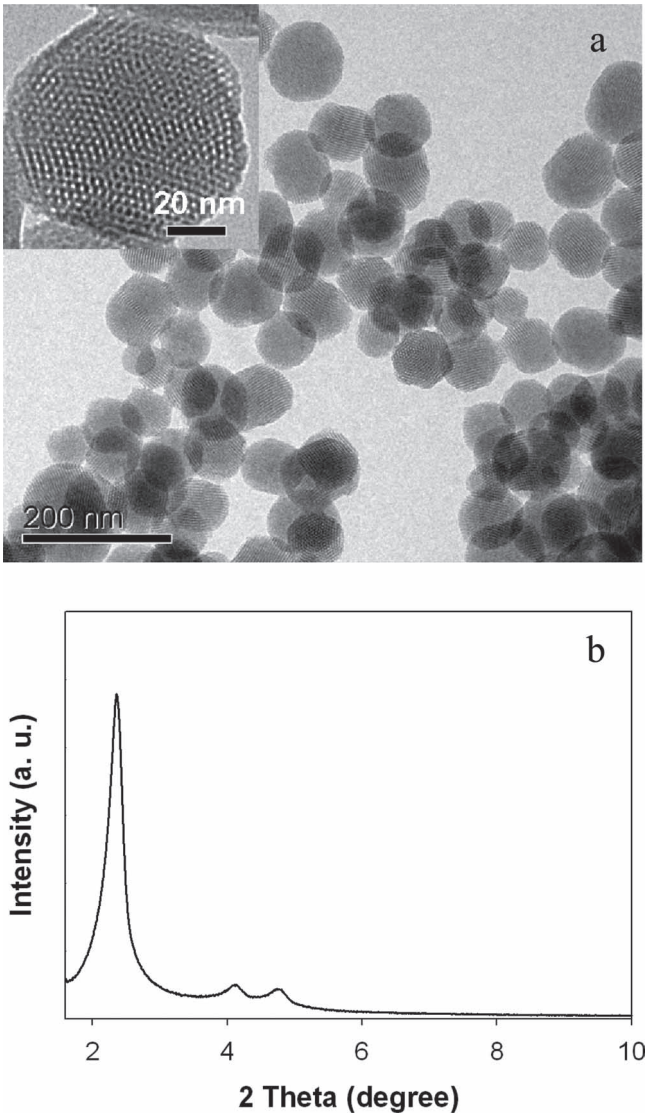

Figure 1. a) TEM images and b) powder X-ray pattern of as-synthesized MSN-Cl.

measurements. TEM images showed that the resulting spherical MSN-Cl had a diameter of ≈80 nm and a typical hexagonally channel-like pore (**Figure 1**a). The XRD of siliceous MCM-41 as-synthesized showed three low-angle reflections typical of a hexagonal array that could be indexed as (100), (110) and (200) Bragg peaks with an a_0 cell parameter of 4.1 Å (Figure 1b). Moreover, the MSN-Cl particles had a surface area of 1096 $m^2\ g^{-1}$, a narrow pore distribution, and an average pore diameter of 3.04 nm (**Figure 2** black circles). The as-prepared MSN-Cl was then treated with sodium azide in *N*,*N*-dimethylformamide (DMF) to give an azide-carrying surface (MSN-N_3). After azide activation, the DNA oligomers were subsequently attached to the MSN surface using a click chemistry approach.[13] Detailed DNA sequence, modification, and linkages were shown in the Experimental Section. The successful conversion of MSN surface was confirmed by FTIR spectroscopy. As shown in **Figure 3**, the sample MSN-Cl only showed the silica framework vibrations,

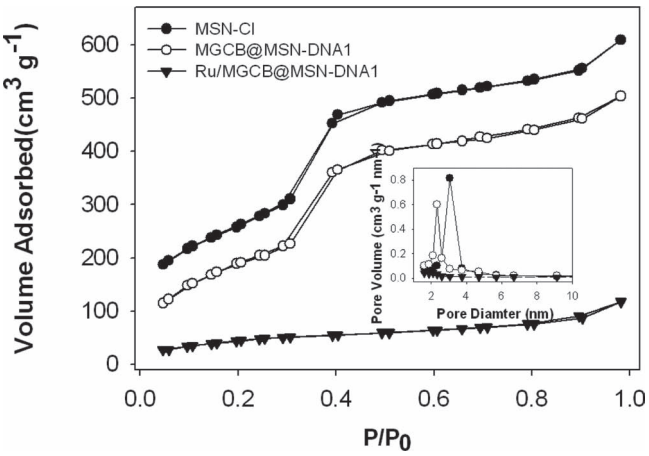

Figure 2. Nitrogen sorption isotherms and pore size distributions (inset) of MSN-Cl (black circles), MGCB@MSN-DNA1 (open circles), and Ru/MGCB@MSN-DNA1 (black triangles).

whereas the sample MSN-N_3 exhibited the characteristic azide stretch signal at 2110 cm^{-1} (see the dotted line in Figure 3). After DNA attachment, this band at 2110 cm^{-1} was strongly reduced in intensity. We had taken this result as evidence for the covalent DNA binding to the MSN surface. Quantification of DNA anchored on MSN surface was determined by a UV–vis spectroscopy to be approximately 4.3 μmol g^{-1} SiO_2.

To achieve the goal of light-controllable release, the MSN-DNA1 was soaked in a solution of MGCB to permit the light-induced hydroxide ion emitter to diffuse into the pores of the MSN and then immobilize on the pore wall through strong hydrophobic interaction between MGCB molecules and silanes. The obtained particles were then repeated washing with a phosphate-buffered saline (PBS) buffer solution (pH = 7.2). The successful loading of MGCB was confirmed by N_2 adsorption–desorption isotherm (Figure 2 open circles) and UV–vis spectroscopy (Figure S1 and Figure S2, Supporting Information). Compared with the sample MSN-DNA1 (a surface area of 813 m^2 g^{-1}), the surface area of the sample MGCB@MSN-DNA1 reduced by ≈26%. On the other hand, practically similar pore sizes were determined with value of 2.34 nm for sample MGCB@MSN-DNA1, indicating that the residual porosity remaining in MGCB@MSN-DNA1 had little effect on the guest loading. The UV–vis spectrum of MGCB@MSN-DNA1 displayed apparent absorption band around 620 nm corresponding to the absorption band of free MGCB (Figure S1, Supporting Information). However, the MSN-DNA1 had no absorption band around 620 nm. In addition, the colours of particles before and after incubation with MGCB became from ivory white to blue (Figure S2, Supporting Information). These results confirmed that the MGCB was loaded into the pores of MSN, and the loading amount was determined to be as high as 41 μmol g^{-1} SiO_2 by UV–vis spectroscopy. Moreover, to show that the entrapped MGCB was not released by diffusion even upon opening of the pores, the UV–vis spectra of supernatants of MGCB@MSN-DNA1 were investigated at PBS buffer solution (pH = 7.2). Figure S3,S4 (Supporting Information) showed a negligible release at both dark and UV light, indicating that both MGCB and MG cation could be stably immobilized into the pores of MSN through strong hydrophobic interaction between MGCB molecules and silanes and electrostatic attraction between MG cations and abundant deprotonated silanol groups (Si–O^-).

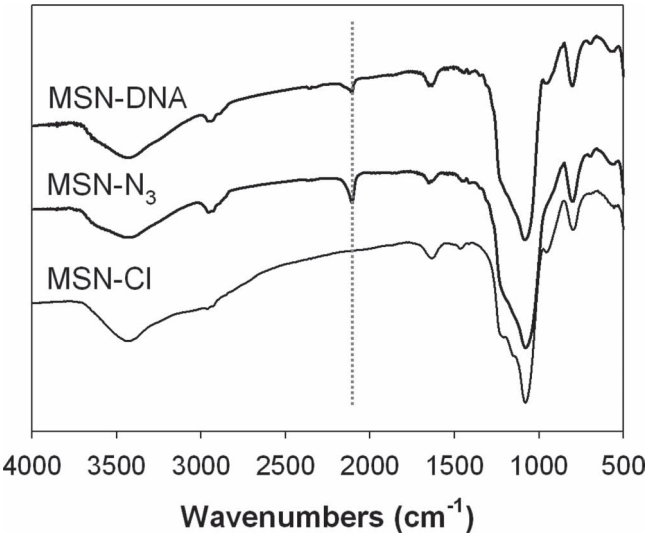

Figure 3. FTIR spectra of the samples MSN-Cl, MSN-N_3, and MSN-DNA.

To clearly show the controlled release behavior, $Ru(bipy)_3^{2+}$ molecules were selected as guests and loaded into the mesopores of MGCB@MSN-DNA1. The pore closure was performed by the formation of i-motif structures when the pH in the solution was adjusted to 5.0. The excess guests were removed by centrifugation and repeated washing with aqueous solution (pH = 5.0). The N_2 adsorption–desorption isotherm of the $Ru(bipy)_3^{2+}$-loaded MGCB@MSN-DNA1, denoted as Ru/MGCB@MSN-DNA1, was typical for mesoporous systems with filled mesopores (Figure 2 black triangles). This sample showed flat curves when compared to those of the MCM–41 parent materials at the same scale, thus indicating significant pore blocking and the subsequent absence of appreciable porosity. The UV–vis spectrum of Ru/MGCB@MSN-DNA1 exhibited apparent enhancement of absorption band around 488 nm (Figure S1, Supporting Information). At the same time, the colour of compound showed green due to merge blue and red (Figure S2, Supporting Information). These results provided direct evidence of the high content of guests filling the pores. From UV–vis spectroscopy analysis, the $Ru(bipy)_3^{2+}$ molecules content of Ru/MGCB@MSN-DNA1 was calculated to be 53 μmol g^{-1} SiO_2.

According to the report in previous literature,[18] we knew that UV light could directly result in remarkable pH increase in the solution containing MGCB. To investigate this change when MGCB was immobilized on pore wall of MSN before loading with $Ru(bipy)_3^{2+}$ molecules, the photoirradiated pH-jump of solution containing Ru/MGCB@MSN-DNA1 (1.0 mg mL^{-1}) was thus measured by a pH meter. Multiple cycling of pH value in this system was successfully achieved by turning the UV light on and off alternately. **Figure 4** showed the light-induced pH changes in initial aqueous solution (pH = 4.93)

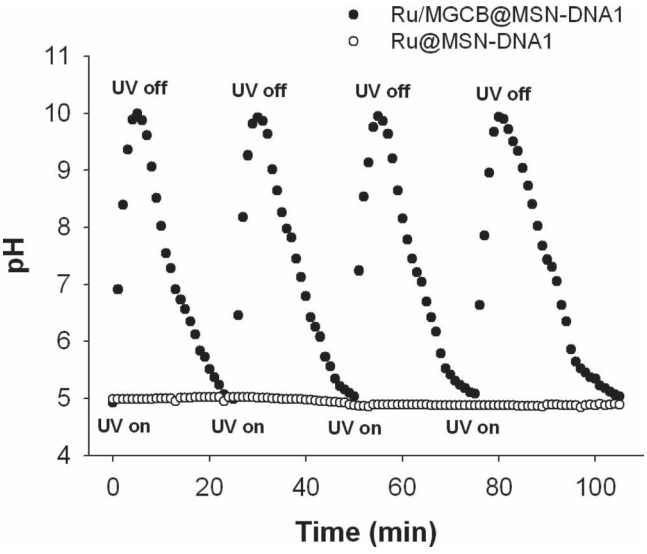

Figure 4. Monitoring of the cycling of the switch of pH value by pH meter. The control experiment in the absence of MGCB shows no change of the pH value after each cycle of UV irradiation.

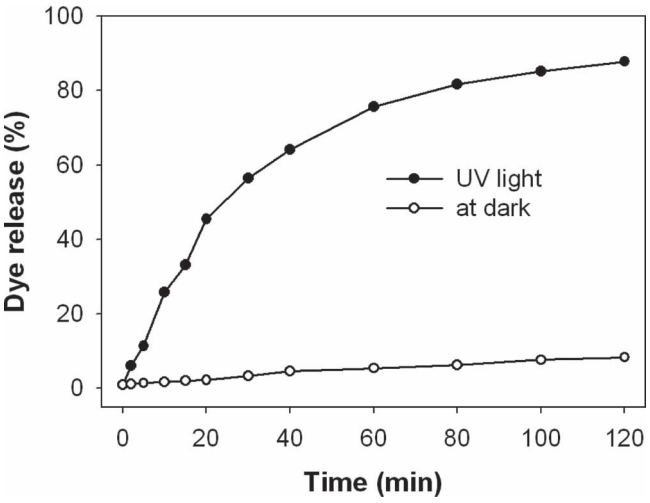

Figure 5. Release profiles of $Ru(bipy)_3^{2+}$ molecules from Ru/MGCB@MSN-DNA1 in the dark and with UV light.

containing the Ru/MGCB@MSN-DNA1. Obviously, the pH increased from 4.93 to 10.09 by photoirradiation. After removal of the light, the pH returned to the initial value after 20 min in dark. The cycle, an increase in pH by photoirradiation and a return in dark, could be repeated several times. Moreover, over 3 cycles the decrease in the amplitude of the system was inconspicuous. Evidently, the repeated photoirradiation did not affect the photoactivity of MGCB immobilized on pore wall of MSN. However, no change in pH was detected in the solution containing $Ru(bipy)_3^{2+}$-loaded MSN-DNA1 (Ru@MSN-DNA1). These results presented unambiguous evidence that photoirradiation could change the pH value of the solution containing Ru/MGCB@MSN-DNA1 and then the multiple cycling of pH value was ascribable to photodissociation of the MGCB. Furthermore, the system after irradiation multiple times could be used to load the $Ru(bipy)_3^{2+}$ molecules again, indicating that the nucleic acids on the surface of MSN remained intact after irradiation with low-intensity UV light (≈0.2 W cm^{-2}) for several times.

The photon-fueled controlled-release profiles were then investigated by plotting fluorescence intensities of $Ru(bipy)_3^{2+}$ at the emission maximum (594 nm) as a function of time. As shown in **Figure 5**, the emission intensity of $Ru(bipy)_3^{2+}$ in supernatant was essentially constant in dark, thus indicating that i-motif DNA acted as an efficient cap for retention of guest molecules with negligible leakage. On the contrary, the presence of 365 nm UV light induced cargo release from pores and 83% release was obtained after 2 h. In addition, the UV–vis spectrum of Ru/MGCB@MSN-DNA1 after the release of entrapped $Ru(bipy)_3^{2+}$ and washing for several times still exhibited obvious absorption band at 620 nm (Figure S5, Supporting Information). And the colour of the washed Ru/MGCB@MSN-DNA1 suspension after $Ru(bipy)_3^{2+}$ release still retained blue (Figure S6, Supporting Information). These results also indicated that $Ru(bipy)_3^{2+}$ could diffuse from pores of MSN into supernatant and MGCB could hardly escape from the pores under the release process. In comparison, the results of control DNA (DNA2)-functionalized MSN (Ru/MGCB@MSN-DNA2) showed remarkable guests liberation in both dark and photoirradiation (**Figure 6**a). However, Ru@MSN-DNA1 showed a low release under same conditions (Figure 6b), due to no change in pH value. These data clearly demonstrated that we were able to close the pores of MSN with i-motif DNA, and to release the loaded guest molecules subsequently by the unfolding of i-motif DNA as a result of light-triggered pH increase. In addition, we measured the luminescence properties of $Ru(bipy)_3^{2+}$ in the presence of 365 nm light (Figure S7, Supporting Information). The results showed that photoirradiation had no effect on the luminescence properties of $Ru(bipy)_3^{2+}$.

Owing to the reversible DNA1 conformation switches between i-motif structure and single-stranded form, it was possible that the release of guest molecules in small portions was achieved. As a proof of concept, a partial release of $Ru(bipy)_3^{2+}$ could be regulated with open–closed cycles by turning the UV light on and off alternately. As showed in **Figure 7**, the closed state strongly constrained the release of the guest molecules in dark. In contrast, an obvious release of the entrapped $Ru(bipy)_3^{2+}$ molecules was triggered in the open state as a result of the unfolding of i-motif DNA when the UV light source was suddenly turned on (see the arrow in Figure 7). After 20 min, the release of the entrapped $Ru(bipy)_3^{2+}$ was restricted again by turning the UV light off. This inhibition was slower than the process when the release was triggered. The variation in time might be ascribed to the difference in the folding and unfolding rates of i-motif DNA grafted on the surface of MSN. After another 50 min, the UV light was turned on again and further released the entrapped $Ru(bipy)_3^{2+}$ molecules until the UV light was turned off. The results indicated that the partial release of guest molecules could be operated at will. For investigating the feasible applications, the cytotoxicity caused by irradiation of 365 nm light (0.2 W cm^{-2}) was demonstrated. As shown in Figure S8 (Supporting Information), the cytotoxicity of the light against HeLa cells increased with the increase of

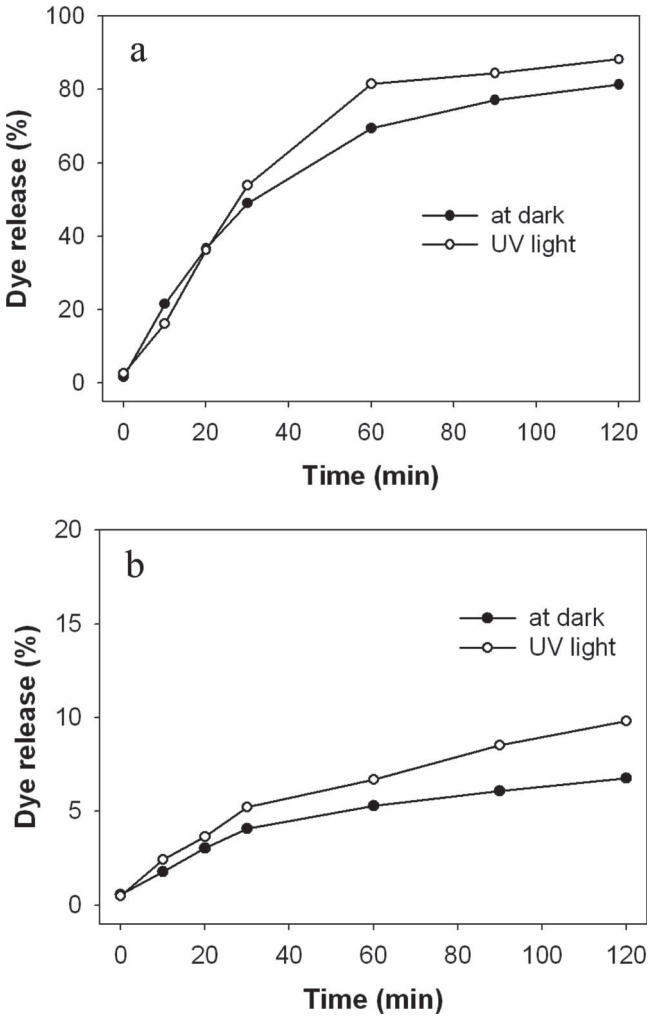

Figure 6. a) Release profiles of $Ru(bipy)_3^{2+}$ from Ru/MGCB@MSN-DNA2 in the dark and with UV light. b) Release profiles of $Ru(bipy)_3^{2+}$ from Ru@MSN-DNA1 in the dark and with UV light.

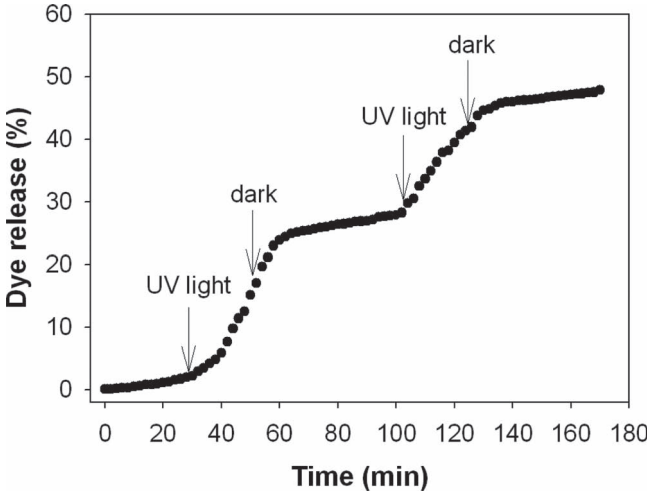

Figure 7. Partial release profile of $Ru(bipy)_3^{2+}$ from Ru/MGCB@ MSN-DNA1 as function of light variations.

irradiation time. After irradiation for 2 h, the cell viability is 91%, indicating no obvious cytotoxic effect.

3. Conclusions

In summary, we have first designed and synthesized a novel photon-fueled controlled release vehicle using photoirradiated pH-jump system mediated conformational switch of i-motif DNA. In this system, MGCB was immobilized on pore walls of MSN as the reversible light-induced hydroxide ion emitter and i-motif DNA was grafted on the surface of MSN as cap material. The $Ru(bipy)_3^{2+}$ molecules as model guests had been encapsulated into pores of MSN by using i-motif DNA caps in dark. The release profile was strongly dependent on the unfolding of i-motif DNA due to the MGCB-mediated pH increase of solution in the presence of UV light. Furthermore, the photon-fueled controlled release system was reversible, and the entrapped guest molecules could be delivered in small portions by turning the UV light on and off alternately. This proof of concept might not only promote the application of DNA molecules but also open a door to constructing various photon-fueled controlled release nanodevices by using a combination of some photoirradiated pH-jump systems (e.g., MGCB or compounds containing ArOH) and other kinds of pH-sensitive caps (acetal linker, boronate ester, pH-sensitive supramolecular nanovalve, pH-dependent polymer, etc.).

4. Experimental Section

Reagents and Materials: Tris(benzyltriazolylmethylamine) ligand, methyltrimethoxysilane (MTMS), $[Ru(bipy)_3]Cl_2$ (bipy = 2,2′-bipyridine), 3-[4,5-dimethylthialzol-2-yl]-2,5-diphenyltetrazo-lium bromide (MTT) and molecular malachite green carbinol base (MGCB) were purchased from Sigma-Aldrich. CuBr (99.9%), tris(hydroxymethyl)-aminomethane (Tris), *N*-cetyltrimethylammonium bromide (CTAB) and 3-chloropropyltrimethoxysilane (ClTMS) were purchased from Alfa Aesar. Sodium azide (NaN_3, 99%) and ascorbic acid were purchased from Dingguo reagent company (Beijing, China). Sodium hydroxide (NaOH), ammonium hydroxide solution (25%), *N*,*N*-dimethylformamide (DMF), dimethyl sulfoxide (DMSO), mesitylene, tert-butyl alcohol (tBuOH), toluene, trisodium citrate dihydrate and tetraethylorthosilicate (TEOS, 28%) were obtained from Xilong reagent company (Guangdong, China). Nanopure water (18.2 MΩ; Millpore Co., USA) was used in all experiments and to prepare all buffers. All the chemicals were used as received without further purification. The oligonucleotides were obtained by Sangon Biotechnology Inc. (Shanghai, China). The sequences are as follows: DNA1: 5′ -Alkyne-$(CH_2)_4$-CCC TAA CCC TAA CCC TAA CCC-3′ and DNA2: 5′ -Alkyne-$(CH_2)_4$-CTC TCA CTC TCA CTC TCC ACC-3′.

Synthesis of Mesoporous Silica Nanoparticles (MSN): Large pore diameter MSN samples, with hexagonal well-ordered pore structures, were synthesized under low concentration precursor (TEOS), surfactant (CTAB), and a base catalyst (NH_4OH), in a two-step preparation. The sol–gel process, for the co-condensation of TEOS to synthesize MSN, was as follows. First, CTAB (0.50 g, 1.4 mmol) was dissolved in NH_4OH solution (240 mL, 0.51 M) at 313 K and then the structural swelling agent mesitylene (4.0 g, 33 mmol) was added. After stirring for 1 h, 4.0 mL of mixture containing MTMS organosilane (0.1 M) and TEOS (0.2 M) in ethanol was added, and the solution stirred for an additional 2 h. Then, the further co-condensation took place through the slow addition of high concentration TEOS (4.0 mL, 1.0 M in ethanol), under vigorous stirring for another 2 h. This solid crude product was subsequently collected by centrifugation at 10 000 rpm for 10 min, washed with deionized water

and ethanol several times, and dried under high vacuum to yield the as-synthesized MSN.

Chemical Modification of the MSN Surface: The as-synthesized MSN (0.50 g) was refluxed for 20 h in 40.0 mL of anhydrous toluene with ClTMS (0.50 mL) to yield the 3-chloropropyl-functionalized MSN (MSN-Cl) material. The MSN-Cl nanoparticles were then collected by centrifugation, washed thoroughly with toluene and ethanol, and dried in vacuum. To remove the surfactant template (CTAB), MSN-Cl particles (0.40 g) were refluxed for 6 h in an ethanolic solution (70 mL) containing HCl (0.70 mL, 37.2%). The resulting material was separated by centrifugation and extensively washed with nanopure water and ethanol. The surfactant-free MSN-Cl material was placed under high vacuum with heating at 333 K to remove the remaining solvent from the mesopores. The MSN-Cl (0.20 g) was added to a saturated solution of sodium azide in N,N-dimetylformamide (DMF, 20 mL) solution and stirred at 90° for 12 h. The resulting mixture was separated by centrifugation, redispersed in PBS buffer solution, and stirred for 6 h to remove remaining DMF from the mesopores. After purification, the azide-functionalized nanoparticles (MSN-N_3) were washed with water and ethanol before being dried in vacuum.

Grafting of Alkyne-Modified DNA to MSN-N_3: TheMSN-N_3 particles (2.0 mg) were dispersed in 200 µL of aqueous solution containing alkyne-modified single-stranded DNA (65.0 µM). In a separate vial, CuBr solution (1 µL, 0.1 M in DMSO/tBuOH 3:1) and the tris(benzyltriazolylmethylamine) ligand (2 µL, 0.1 M in DMSO/tBuOH 3:1) were mixed and added to the DNA-particle mixture, which was then stirred overnight at room temperature. The resulting particles were washed three times with water via centrifugation. Subsequently, the particles were dried under high vacuum to yield the DNA-functionalized MSN (MSN-DNA). The quantification of left DNA was accomplished by UV–vis spectroscopy to be 4.4 nmol, which corresponded to an immobilization amount of 4.3 µmol g^{-1} SiO_2.

MGCB Immobilizing Experiments: The purified MSN-DNA1 (1.5 mg) was incubated in ethanol containing MGCB (0.5 mg, 1.4 mmol) at 20° overnight, followed by centrifuging and washing with deionized water to afford MGCB-immobilized MSN-DNA1 (MGCB@MSN-DNA1). The redundant MGCB was monitored via the absorbance band of the dye centered at 620 nm. The loading amount of MGCB was calculated to be 41 µmol g^{-1} SiO_2.

Ru(bipy)$_3^{2+}$ Loading: The pores of MGCB@MSN-DNA1 (1.5 mg) were further diffusion-filled with cargo molecules by immersing the articles in a solution of Ru(bipy)$_3^{2+}$ (200 µL, 0.10 M, pH = 7.2) for 12 h. The pH value of the suspension was adjusted to 5.0 by the addition of HCl. The solution was stirred for 6 h, followed by centrifuging and repeated washing with citrate buffer (25 mM, pH = 5.0) to remove residual Ru(bipy)$_3^{2+}$ molecules from the exterior surface of the material. All the washing solutions were collected and the loading of Ru(bipy)$_3^{2+}$ was calculated from the difference in the concentration of the initial and left guests to be 53 µmol g^{-1} SiO_2.

Ru(bipy)$_3^{2+}$ Release: A small sample of the Ru(bipy)$_3^{2+}$-loaded MGCB@MSN-DNA1 (Ru/MGCB@MSN-DNA1) was placed in a cuvette, which was then carefully filled with an aqueous solution (200 µL, pH = 5.0). Subsequently, the sample was exposed to 365 nm light (≈0.2 W cm^{-2}) to release the entrapped Ru(bipy)$_3^{2+}$ molecules. The release profiles of Ru(bipy)$_3^{2+}$ molecules from the pores to aqueous solution was monitored via the fluorescence intensity of the dye centered at 594 nm.

Cytotoxicity Assay: The cytotoxicity caused by irradiation of 365 nm light was investigated by MTT assay. For the MTT assay, HeLa cells were seeded into 96-well plates and grown overnight. The cells were then incubated with irradiation at 365 nm for different times (0, 10, 30, 60, 120 min). Afterwards, cells were incubated in media containing MTT (0.5 mg mL^{-1}) for 3 h. The precipitated formazan violet crystals were dissolved in DMSO (150 µL) at 37 °C. The absorbance was measured at 490 nm by multi-detection microplate reader.

Characterization Techniques: Transmission electron microscopy (TEM) image was obtained on a JEOL 3010 microscope and an accelerating voltage of 100 kV. UV–vis spectra were collected using a DU-800. Small-angle powder X-ray diffraction pattern of the MSN materials was obtained in a Scintag XDS-2000 powder diffractometer using CuKα irradiation (λ = 0.154 nm). N_2 adsorption–desorption isotherm was obtained at 77 K on a Micromeritics ASAP 2010 sorptometer by static adsorption procedures. Samples were degassed at 373 K and 10^{-3} Torr for a minimum of 12 h prior to analysis. Brunauer–Emmett–Teller (BET) surface area was calculated from the linear part of the BET plot according to IUPAC recommendations. Pore size distribution was estimated from the adsorption branch of the isotherm by the Barrett–Joyner–Halenda (BJH) method. All fluorescence spectra were recorded on a Hitachi F-4500 FL Spectrophotometer.

Supporting Information

Supporting Information is available from the Wiley Online Library or from the author.

Acknowledgements

This work was supported in part by the Project of Natural Science Foundation of China (90606003, 21175039, 20905023 and 21190044), International Science & Technology Cooperation Program of China (2010DFB30300), Key Technologies Research and Development Program of China (2011AA02a114), Research Fund for the Doctoral Program of Higher Education of China (20110161110016) and project supported by Hunan Provincial Natural Science Foundation and Hunan Provincial Science and Technology Plan of China (10JJ7002, 2011FJ2001).

Received: May 17, 2012
Published online: June 29, 2012

[1] a) A. P. Wight, M. E. Davis, *Chem. Rev.* **2002**, *102*, 3589; b) G. Kickelbick, *Angew. Chem.* **2004**, *116*, 3164; *Angew. Chem. Int. Ed.* **2004**, *43*, 3102; c) F. Hoffmann, M. Cornelius, M. Morell, M. Fröba, *Angew. Chem.* **2006**, *118*, 3290; *Angew. Chem. Int. Ed.* **2006**, *45*, 3216.

[2] a) S. Angelos, Y.-W. Yang, N. M. Khashab, J. F. Stoddart, J. I. Zink, *J. Am. Chem. Soc.* **2009**, *131*, 11344; b) E. Aznar, M. D. Marcos, R. Martínez-Máñez, F. Sancenón, J. Soto, P. Amorós, C. Guillem, *J. Am. Chem. Soc.* **2009**, *131*, 6833.

[3] a) S. Angelos, Y. W. Yang, K. Patel, J. F. Stoddart, J. I. Zink, *Angew. Chem.* **2008**, *120*, 2254; *Angew. Chem. Int. Ed.* **2008**, *47*, 2222; b) L. Du, S. Liao, H. A. Khatib, J. F. Stoddart, J. I. Zink, *J. Am. Chem. Soc.* **2009**, *131*, 15136; c) Y.-L. Zhao, Z. Li, S. Kabehie, Y. Y. Botros, J. F. Stoddart, J. I. Zink, *J. Am. Chem. Soc.* **2010**, *132*, 13016.

[4] a) Y.-Z. You, K. K. Kalebaila, S. L. Brock, D. Oupicky, *Chem. Mater.* **2008**, *20*, 3354; b) Q. Fu, G. V. R. Rao, L. K. Ista, Y. Wu, B. P. Andrzejewski, L. A. Sklar, T. L. Ward, G. P. López, *Adv. Mater.* **2003**, *15*, 1262.

[5] a) E. Climent, A. Bernardos, R. Martínez-Máñez, A. Maquieira, M. D. Marcos, N. P. Navarro, R. Puchades, F. Sancenón, J. Soto, P. Amorós, *J. Am. Chem. Soc.* **2009**, *131*, 14075; b) Y. Zhao, B. G. Trewyn, I. I. Slowing, V. S.-Y. Lin, *J. Am. Chem. Soc.* **2009**, *131*, 8398.

[6] a) A. Schlossbauer, J. Kecht, T. Bein, *Angew. Chem.* **2009**, *121*, 3138; *Angew. Chem. Int. Ed.* **2009**, *48*, 3092; b) C. Coll, L. Mondragón, R. Martínez-Máñez, F. Sancenón, M. D. Marcos, J. Soto, P. Amorós, E. Pérez-Payá, *Angew. Chem.* **2011**, *123*, 2186; *Angew. Chem. Int. Ed.* **2011**, *50*, 2138.

[7] a) C.-Y. Lai, B. G. Trewyn, D. M. Jeftinija, K. Jeftinija, S. Xu, S. Jeftinija, V. S.-Y. Lin, *J. Am. Chem. Soc.* **2003**, *125*, 4451; b) B. G. Trewyn,

I. I. Slowing, S. Giri, H.-T. Chen, V. S.-Y. Lin, *Acc. Chem. Res.* **2007**, *40*, 846.

[8] a) F. Torney, B. G. Trewyn, V. S.-Y. Lin, K. Wang, *Nat. Nanotechnol.* **2007**, *2*, 295; b) J. L. Vivero-Escoto, I. I. Slowing, C.-W. Wu, V. S.-Y. Lin, *J. Am. Chem. Soc.* **2009**, *131*, 3462.

[9] a) N. K. Mal, M. Fujiwara, Y. Tanaka, *Nature* **2003**, *421*, 350; b) R. Liu, X. Zhao, T. Wu, P. Feng, *J. Am. Chem. Soc.* **2008**, *130*, 14418; c) J. Lai, X. Mu, Y. Xu, X. Wu, C. Wu, C. Li, J. Chen, Y. Zhao, *Chem. Commun.* **2010**, *46*, 7370.

[10] a) T. D. Nguyen, H. R. Tseng, P. C. Celestre, A. H. Flood, Y. Liu, J. F. Stoddart, J. I. Zink, *Proc. Natl. Acad. Sci. USA* **2005**, *102*, 10029; b) T. D. Nguyen, K. C. F. Leung, M. Liong, Y. Liu, J. F. Stoddart, J. I. Zink, *Adv. Funct. Mater.* **2007**, *17*, 2101.

[11] E. Climent, R. Martínez-Máñez, F. Sancenón, M. D. Marcos, J. Soto, A. Maquieira, P. Amorós, *Angew. Chem.* **2010**, *122*, 7439; *Angew. Chem. Int. Ed.* **2010**, *49*, 7281.

[12] C. Chen, F. Pu, Z. Huang, Z. Liu, J. Ren, X. Qu, *Nucleic Acids Res.* **2011**, *39*, 1638.

[13] C. Chen, J. Geng, F. Pu, X. Yang, J. Ren, X. Qu, *Angew. Chem.* **2011**, *123*, 912; *Angew. Chem. Int. Ed.* **2011**, *50*, 882.

[14] V. Özalp, T. Schäfer, *Chem. Eur. J.* **2011**, *17*, 9893.

[15] a) K. Hamad-Schifferli, J. J. Schwartz, A. T. Santos, S. Zhang, J. M. Jacobson, *Nature* **2002**, *415*, 152; b) L. Kröck, A. Heckel, *Angew. Chem.* **2005**, *117*, 475; *Angew. Chem. Int. Ed.* **2005**, *44*, 471; c) A. Heckel, G. Mayer, *J. Am. Chem. Soc.* **2005**, *127*, 822; d) M. Zhou, X. Liang, T. Mochizuki, H. Asanuma, *Angew. Chem.* **2007**, *14*, *2567*; *Angew. Chem. Int. Ed.* **2010**, *49*, 2167.

[16] H. Liu, Y. Xu, F. Li, Y. Yang, W. Wang, Y. Song, D. Liu, *Angew. Chem.* **2007**, *14*, 2567; *Angew. Chem. Int. Ed.* **2007**, *46*, 2515.

[17] a) D. Liu, S. Balasubramanian, *Angew. Chem.* **2003**, *115*, 5912; *Angew. Chem. Int. Ed.* **2003**, *42*, 5734; b) D. Liu, A. Bruckbauer, C. Abell, S. Balasubramanian, D.-J. Kang, D. Klenerman, D. Zhou, *J. Am. Chem. Soc.* **2006**, *128*, 2067; c) Y. Mao, D. Liu, S. Wang, S. Luo, W. Wang, Y. Yang, Q. Ouyang, L. Jiang, *Nucleic Acids Res.* **2007**, *35*, e33; d) F. Xia, W. Guo, Y. Mao, X. Hou, J. Xue, H. Xia, L. Wang, Y. Song, H. Ji, Q. Ouyang, Y. Wang, L. Jiang, *J. Am. Chem. Soc.* **2008**, *130*, 8345; e) D. Liu, *NPG Asia Mater.* **2011**, *3*, 109.

[18] a) M. Irie, Y. Hirano, S. Hashimoto, K. Hayashi, *Macromolecules* **1981**, *14*, 262; b) R. N. Manchair, *Photochem. Photobiol.* **1967**, *6*, 779.